Quantitative Analysis of Vortex Flow Patterns in 4D Flow Measurements

Jochen von Spiczak[1], Gérard Crelier[2], Daniel Giese[1], Sebastian Kozerke[2], David Maintz[1], and Alexander Christian Bunck[1]

[1]Department of Radiology and Neuroradiology, University Hospital of Cologne, Cologne, Germany, [2]Institute for Biomedical Engineering, University and ETH Zurich, Zurich, Switzerland

Purpose: 4D flow magnetic resonance imaging (MRI) permits the assessment of volumetric, multi-directional blood flow velocities[1]. Intuitive visualization via stream- and pathlines can be computed from the measured flow field[2]. It has been shown that vortex flow patterns are physiologically present in the heart chambers[3], aorta[4], and pulmonary circulation[5], but can also be correlated to certain pathologies[6,7,8]. In the aorta in particular, a physiological right handed helical flow has been consistently described[4,9]. However, so far, flow pattern characterization has mainly been restricted to a merely qualitative analysis. In first attempts of more quantitative evaluation, velocity values had to be exported from flow analysis software to compute and investigate vorticity separately in a two-dimensional fashion[3,5]. Three-dimensional vortex-cores were identified in previous studies, but neither have been quantified[10]. The objective of this work was to integrate efficient region-of-interest (ROI) based vortex analysis into the evaluation workflow and propose new three-dimensional quantitative parameters for temporal and spatial assessment of swirling flow.

Methods:
<u>Data acquisition:</u> A cohort of 9 healthy subjects was scanned. Time-resolved 3D PC data covering the left-ventricular outflow tract, ascending and descending aorta were acquired on a Philips 3T Achieva system (Philips Healthcare, Best, The Netherlands). Scan parameters of the respiratory navigated and retrospectively ECG triggered sequence were: FOV = 320x256x46 mm^3, matrix = 160x160x20, SENSE reduction factor = 2, TR = 3.05-3.94 ms, flip angle = 5°, $Venc_{x,y}$ = 200 cm/s, $Venc_z$ = 100 cm/s, cardiac phases = 25, resulting scan resolution = 2.3x2.3x2.3 mm^3. 3 patients with dilated ascending aortas were scanned (patient 1: 36.1x32.7 mm aortic diameter, patient 2: 39.3x35.0 mm, patient 3: 46.3x45.7 mm). For patient 3, adapted scan parameters included: FOV = 350x280x75 mm^3, matrix = 176x176x30, TR = 4.10 ms, cardiac phases = 20, $Venc_{x,z}$ = 50 cm/s, $Venc_y$ = 60 cm/s.
<u>Evaluation:</u> For two-dimensional assessment, a standardized set of 5 ROIs was defined for each dataset (Figure 1c), 0: directly above the aortic bulb, 1: horizontal slice through the ascending aorta, 2: proximal to the brachiocephalic artery, 3: between the left common carotid artery and left subclavian artery, 4: distal to the left subclavian artery, 5: axial slice through the descending aorta at the level of ROI 1. For each ROI, a heat-map of time-resolved vorticity values $\vec{\omega} = \nabla \times \vec{v}$ (with $\vec{v}$ being the velocity field) was computed. The evolution of minimum, maximum, and average values throughout the cardiac cycle was analyzed. For three-dimensional analysis, vortex-core detection was implemented following an algorithm[11] that combines the predictor-corrector method[12] with $Lambda_2$ correction[13]. The length of the detected vortex-core and its vorticity throughout its course were recorded over time. For intuitive visualization, a set of characteristic streamlines was calculated similar to line predicates[14] as shown in Figure 1a. All techniques described above were implemented in C++ as a separate module inside the commercially available 4D flow software package GTFlow (GyroTools, Zurich, Switzerland).

Results: 3D vortex-core analysis is illustrated in Figure1a/b: as shown, the automatically identified vortex-core follows the maximum vorticity/$Lambda_2$ values and is surrounded by the right-handed helical flow (a). Vorticity strength (averaged over all volunteers) escalates in early systole, followed by an increase of the vortex' length, which reaches an elongation peak in mid systole, before both parameters similarly degrade to overall low values in diastole (b). In Figure 1d, temporal evolution of the average vorticity value in the 5 standardized ROIs is exemplarily illustrated for one healthy subject: helical flow is developed early in the ascending aorta (ROI 0/1) followed by maximum values in mid-systole in the aortic arch (ROI 2/3/4). Figure 1e/f show the altered vortex flow in the dilated aorta of 75 years old patient 3 (aortic diameter 46.3x45.7 mm). Note the temporal and spatial alteration of the complex flow: swirling flow develops lately in mid/end-systole close to the aortic bulb (ROI 0/1/2), the vortex is noticeably weaker, no physiological helical flow is found in the aortic arch. Analysis further indicated that changes get more distinct the wider the aorta dilatation progresses (patient 1 < patient 2 < patient 3).

Discussion/Conclusion: New parameters for quantitative assessment of vortical flow patterns were defined and applied in the analysis of physiological aortic blood flow as well as pathologically altered flow in aortic aneurysms. Both two- and three-dimensional measures were reproducible in all healthy subjects. Vortex-core detection could be used for determining the spatial and temporal vortex dimensions. Vorticity analysis in consecutive, standardized ROIs proved to be useful for locating vortex flow patterns. Future work includes the assessment of how temporal and spatial vortex quantification can help to grade flow related pathologies and their prognosis.

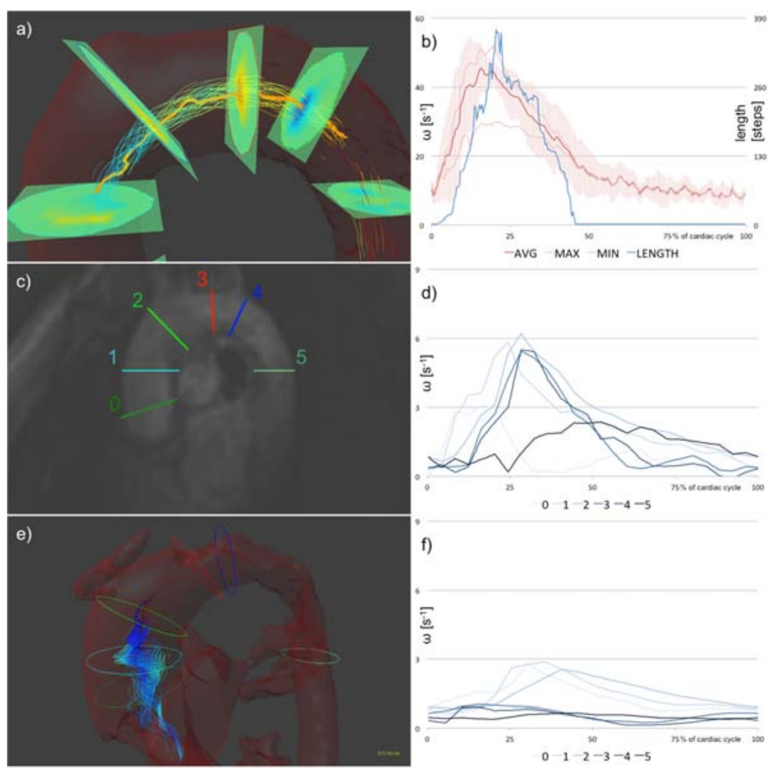

Figure 1: Visualization (a) and quantitative assessment (b) of automatically identified vortex-cores averaged over the 9 healthy subjects in b (standard deviation of average values in light red). Definition of 5 standard ROIs (c) and evolution of their average vorticity values in one exemplary healthy subject (d). Similar plot from the dataset of a 75 years old patient (f) with complex vortex patterns in his dilated ascending aorta (e).

1. Wigstrom L, MRM 1996; 36(5):800-3. 2. Buonocore MH, MRM 1998; 40(2):210-26. 3. Wong KK, Med Eng Phys. 2010; 32(2):174-88. 4. Kilner PJ, Circulation 1993; 88(5 Pt 1):2235-47. 5. Bächler P, MRI 2013; 31(2):178-88. 6. Markl M, Circulation 2007; 116(10):e336-7. 7. Reiter G, Circ Cardiovasc Imaging. 2008; 1(1):23-30. 8. Bissell MM, Circ Cardiovasc Imaging. 2013;6(4):499-507. 9. Frydrychowicz A, Eur Radiol. 2012; 22(5):1122-30. 10. Stalder AF, Proc. 18th ISMRM, 2010. 11. Stegmaier S, Proc. IEEE Conf. Visualization, 2005. 12. Banks DC, IEEE Trans. on Visualization and Computer Graphics, 1(2):151–163, 1995. 13. Jeong J, J. Fluid Mechanics, 285:69–94, 1995. 14. Born S, IEEE Trans Vis Comput Graph, 19(6):900-12, 2013.